METEOR CRATER IMPACT MELT FORMATION: EVIDENCE FOR CARBONATE MELTING. T. A. Gaither, J. J. Hagerty, and A. L. Gullikson. U.S. Geological Survey, Astrogeology Science Center, 2255 N. Gemini Drive, Flagstaff, AZ 86001, email: tgaither@usgs.gov

Introduction: Recent sample analyses and numerical models [e.g., 1-10], indicate that the formation of Meteor Crater was much more complex than previously thought. Current numerical models are insufficient for explaining certain aspects of the impact melting process, target rock-projectile mixing, siderophile element fractionation trends, and ejecta blanket formation processes, and require further investigation to understand newly identified complexities. To address these issues we are exploiting the USGS Meteor Crater Sample Collection, which consists of over 2,500 m of drill cuttings from 161 drill holes into the ejecta blanket of Meteor Crater. We are utilizing these drill cuttings to study the composition and spatial distribution of impact-generated materials associated with the ejecta blanket, in an effort to better understand the complexity of cratering processes and products. Here we focus on recent observations of impact melt particle (IMP) textures and compositions, carbonate inclusion (CI) compositions, and the morphologies of projectile-derived metallic inclusions (MI), and integrating these results with our detailed lithostratigraphic analysis of the ejecta deposits [14].

Methods. We have used a scanning electron microscope (SEM) to document the textures of 37 IMPs from six drill holes within the ejecta blanket (holes 42, 45, 60, 94, 95, 109). We have also determined the composition of a subset of the IMPs (12) via electron microprobe analysis (EMPA). All analyses were done at Northern Arizona University. Each IMP was gently broken into several pieces to expose the particle's interior and mounted under vacuum into an individual epoxy mount. Initial SEM analysis, including energy dispersive spectroscopy (EDS) of IMPs allowed identification of areas of unaltered glass and inclusions (carbonate and metallic) for further EMPA characterization.

Results. *Impact melt textures and compositions.* Observed melt textures are of three types: 1) Crystalline, mostly granular pyroxene groundmass containing MI, CI, and ubiquitous fractured quartz; 2) Near pristine impact melt glass with skeletal olivine crystals, MI, and CI; and 3) Banded glass with MI and CI. The majority of the IMPs display the granular pyroxene groundmass similar to that described by [1]. Vesiculation and particulate carbonate rinds are observed on all types of IMPs. Microprobe spot analyses for pristine glasses (n = 185) indicate a variety of compositions: median values for the major elements SiO_2, CaO, MgO, and FeO are 48 wt%, 7.4 wt%, 11.6 wt%, and 30 wt%, respectively.

Carbonate inclusion textures and compositions. CIs (commonly 50-100 µm, but up to 250 µm) also known as "globules," are observed within all IMPs, but show morphological differences between their host particles. Nearly all granular pyroxene groundmass samples display irregularly shaped, but sometimes spherical, carbonate inclusions in the interstices between the pyroxene crystals; slightly less common are spherical CIs within the near pristine glasses and the banded glasses. One irregularly shaped CI displays 120^o mineral cleavage. Microprobe analyses (n = 341 individual spot analyses) show that the CIs are dominated by calcite compositions with trace to elevated amounts of SiO_2, Al_2O_3, MgO, FeO, and NiO (averages of 4.2, 0.48, 4.6, 0.79, and 0.06 wt%, respectively). MgO is present in nearly all CIs, with concentrations up to 21 wt%. The bulk of the MgO concentrations fall between 1 and 14 wt%, and commonly, individual IMPs have CI compositions spanning this entire range.

Metallic inclusion textures. Most metallic inclusions are 25-100 µm in size, spherical, and display the expected compositional differences described by [5]. Semi-quantitative EDS analysis showed some tabular MIs have compositions consistent with barium sulfate. Submicron-size metallic inclusions were also observed at high magnification. Irregularly shaped high-Z phases were also observed, for the first time, within CIs.

Discussion. The observed impact melt textures and compositions are broadly similar to those described by [1] with the notable exception of the ubiquitous occurrence of the CIs in the groundmass. Determination of whether the CIs are target rock-derived quenched melt products [e.g., 11] or post-impact aqueous alteration products [e.g., 10] is an important question to address and has implications for assessing the pressure and temperature conditions present during the formation of the crater.

We observe three textures of carbonate material associated with the silicate glasses (**Fig. 1**): 1) as particulate, crystalline vesicle fillings and rinds coating the IMP exteriors, similar to [10]; 2) irregularly shaped CIs intermingling with pyroxene-dominated crystalline groundmass, suggestive of immiscible intergrowth during crystallization, similar to [11, 12]; and 3) inclusions within near-pristine and banded glasses, displaying generally spherical shapes with irregular fracture patterns, similar to those described in [9, 11, 12]. The elevated concentrations of SiO_2 and Al_2O_3, within CIs are

significant, as they contrast with the more pure compositions of sedimentary, metamorphic and hydrothermal calcite, which contain no detectable Si or Al [12, 13]. Mg, Fe, and Ni commonly substitute for Ca in calcite, and their presence (especially the metallic blebs within CIs) in the CIs is likely due to contamination from the primary impact melt. For all six melt particles for which both glass and CI compositions were obtained, concentrations of these elements are significantly higher within the groundmass than the CIs.

Based on the textures and compositions observed, we interpret the CIs as Kaibab-derived melt inclusions, rather than aqueous alteration products, and we interpret the textural relationship between the irregularly shaped CIs and the pyroxene groundmass as relict silicate-carbonate liquid immiscibility textures. It seems probable that carbonate melt exsolved from the bulk silicate-carbonate melt (further enriching the melt in SiO_2, Al_2O_3, MgO, FeO, and NiO [i.e., 11]), and crystallized interstitially between pyroxene grains. We suggest that the occurrence of the spherical CIs in the near-pristine and banded glasses is also primary Kaibab-derived melt, and that these melts underwent more rapid quenching than those with granular pyroxene groundmass.

Conclusions and further work. While post-impact carbonate precipitation certainly modified impact melt clasts, the evidence presented here suggests immiscible carbonate melts also participated in the formation of at least some Meteor Crater impact melts. Continuing work includes additional microprobe analyses of melt particles and their inclusions, melt source depth calculations, and analysis of submicron MI on previous interpretations of fractionation processes between projectile and target rock. These results will be combined with our ongoing lithostratigraphic analysis [e.g., 14] of the internal structure of the ejecta blanket to further explore melt formation and ejecta emplacement processes at Meteor Crater.

References: [1] Hörz et al. (2002) *Meteor. Planet. Sci., 37*, 501; [2] Mittlefehldt et al. (2005), *GSA Special Paper*, *384*, 367; [3] Osinski et al. (2008) *Meteor. Planet. Sci., 43*, 1939; [4] Artemieva N. and Pierazzo E. (2011) *Meteor. Planet. Sci., 46*, 805; [5] Gaither et al., (2012) *LPSC 43*, abstract #1601; [6] Hagerty et al. (2012) *75th Ann. Meeting Meteor. Soc.*, abstract #5296; [7] Hagerty et al., (2010) *LPSC 41*, abstract #2213; [8] Hagerty et al., (2011) *PCC* 2, abstract #1109; [9] Osinski et al. (2008) *GSA Special Paper*, *437*, 1; [10] Hörz et al. (2015) *Meteor. Planet. Sci., 50*, 6. [11] Osinski et al. (2015) EPSL 432, 283[12] Osinski and Spray (2001), *EPSL 194*, 17. [13] Deer et al. (1996) Rock-Forming Minerals. Vol. 5B. Non-silicates, Longman Scientific and Technical, Harlow, p. 101. [14] Gullikson et al. (2016) *LPSC 47*.

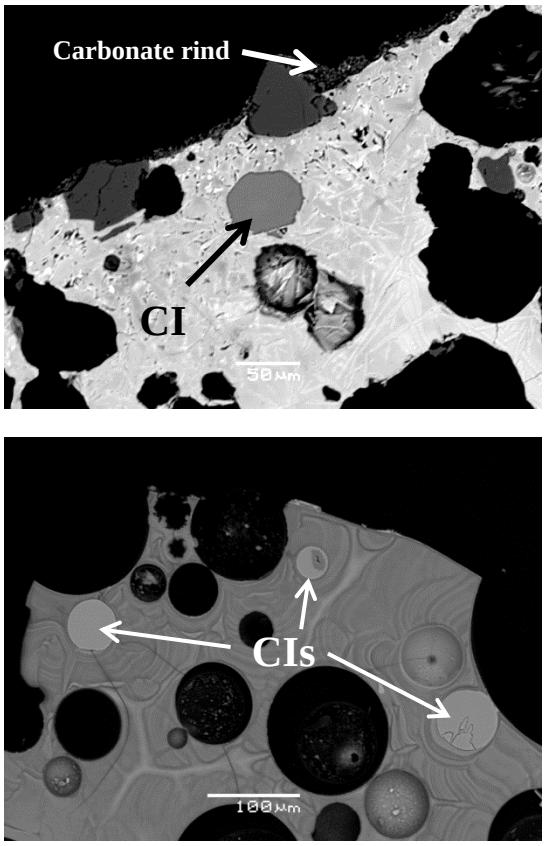

Figure 1. *Top*: SEM BSE image of CI within granular pyroxene groundmass; particulate carbonate rind at top center. *Bottom*: CIs in banded glass. Difference in CI shading between images is due to higher BSE contrast in top image.